J. Ocean Univ. China (Oceanic and Coastal Sea Research)
DOI 10.1007/s11802-017-3213-z
ISSN 1672-5182, 2017 16 (5): 717-726
http://www.ouc.edu.cn/xbywb/
E-mail:xbywb@ouc.edu.cn

Trends in Significant Wave Height and Surface Wind Speed in the China Seas Between 1988 and 2011

ZHENG Chongwei[1), 2), 3), *], ZHANG Ren[1)], SHI Weilai[1)], LI Xin[1)], and CHEN Xuan[1)]

1) *College of Meteorology and Oceanography, People's Liberation Army University of Science and Technology, Nanjing* 211101, *P. R. China*
2) *Key Laboratory of Renewable Energy, Chinese Academy of Sciences, Guangzhou* 510640, *P. R. China*
3) *Dalian Naval Academy, Dalian* 116018, *P. R. China*

(Received May 30, 2016; revised March 5, 2017; accepted June 5, 2017)
© Ocean University of China, Science Press and Springer-Verlag Berlin Heidelberg 2017

Abstract Wind and waves are key components of the climate system as they drive air-sea interactions and influence weather systems and atmospheric circulation. In marine environments, understanding surface wind and wave fields and their evolution over time is important for conducting safe and efficient human activities, such as navigation and engineering. This study considers long-term trends in the sea surface wind speed (WS) and significant wave height (SWH) in the China Seas over the period 1988–2011 using the Cross-Calibrated Multi-Platform (CCMP) ocean surface wind product and a 24-year hindcast wave dataset obtained from the WAVEWATCH-III (WW3) wave model forced with CCMP winds. The long-term trends in WS and SWH in the China Seas are analyzed over the past 24 years to provide a reference point from which to assess future climate change and offshore wind and wave energy resource development in the region. Results demonstrate that over the period 1988–2011 in the China Seas: 1) WS and SWH showed a significant increasing trend of $3.38\,\mathrm{cm\,s^{-1}\,yr^{-1}}$ and $1.52\,\mathrm{cm\,yr^{-1}}$, respectively; 2) there were notable regional differences in the long-term trends of WS and SWH; 3) areas with strong increasing trends were located mainly in the middle of the Tsushima Strait, the northern and southern areas of the Taiwan Strait, and in nearshore regions of the northern South China Sea; and 4) the long-term trend in WS was closely associated with El Niño and a significant increase in the occurrence of gale force winds in the region.

Key words wind speed; significant wave height; climatic change; El Niño; gale occurrence

1 Introduction

Concerns about climate change, its effects on the environment, and the possibility of a power resource crisis in the near future have intensified in recent years. Observations indicate that Earth is undergoing a period of rapid change: global mean surface temperature increased by 0.08–0.14℃ per decade over the period between 1951 and 2012 (IPCC, 2013) and mean global sea level rose by about $1.7\,\mathrm{mm\,yr^{-1}}$ between 1870 and 2004, with the rate of increase intensifying over the past ten years (Church and White, 2006).

Changes in ocean systems generally occur over much longer time periods than those in the atmosphere, and long-term trends in key marine variables (such as WS and SWH) can thus be analyzed as indicators of climate change. Analysis of associated records can assist in informing future efforts in mitigating the negative environmental impacts of climate change on marine environments and coastal areas, such as damage resulting from strong winds and high waves (Zieger, 2010; Carniello *et al.*, 2011; Das and Crepin, 2013; Reza *et al.*, 2017). Moreover, gaining a detailed understanding of wind and waves and their interactions is vital to enable safe and efficient human activities in the marine environment, such as engineering, navigation, and for offshore electricity generation through the harnessing of wind and wave energy (Zheng *et al.*, 2015; Mirab *et al.*, 2015; Mohapatra, 2016; Li and Dong, 2016; Amiri *et al.*, 2016; Behzad and Panahi, 2017; Zheng and Li, 2017; Zheng *et al.*, 2017).

Several previous studies have analyzed the long-term trends of WS and SWH and have provided results for specific regions or those that are averaged globally. For example, Ward and Hoskins (1996) concluded that long-term changes in WS are not significant near the equator but that a decreasing trend exists across the tropical South Atlantic and subtropical North Pacific. Using archived ship reports, Thomas *et al.* (2008) showed that over most of the global ocean there was an increase in estimated speeds of spatially averaged winds of $40\,\mathrm{cm\,s^{-1}\,decade^{-1}}$ ($6\%\,\mathrm{decade^{-1}}$) and $20\,\mathrm{cm\,s^{-1}\,decade^{-1}}$ ($3\%\,\mathrm{decade^{-1}}$) for measured speeds between 1982 and 2002. In addition, Mei *et al.* (2010) found that WS southeast of the Indochina Peninsula (15°–17.5°N, 115°–117.5°E) increased significantly between 1958 and 2001. Furthermore, Sun *et al.*

* Corresponding author. E-mail: chinaoceanzcw@sina.cn

?1994-2017 China Academic Journal Electronic Publishing House. All rights reserved. http://www.cnki.net

(2010) determined that wind speed increased significantly over most of the East China Sea between 1999 and 2008.

Gulev and Grigorieva (2006) used International Comprehensive Ocean-Atmosphere (ICOADS) data to determine a significant increase in SWH of 10–40 cm decade^{-1} over the previous 45 years in both the North Atlantic and North Pacific mid-latitudes, and concluded that the changing patterns in wind sea, swell, and SWH in the North Pacific had become more consistent with one another. Using a 57-yr hindcast (1953 to 2009) obtained from a spectral wave model and forced with reanalysis wind fields, Dodet *et al*. (2010) found a significant increasing trend in SWH of up to 20 cm decade^{-1} in the northeast Atlantic. They also reported a strong positive correlation between SWH and the North Atlantic Oscillation (NAO) index at northern latitudes. Semedo *et al*. (2011) showed a significant increase in SWH of about 12–20 cm decade^{-1} over most of the North Pacific and North Atlantic between 1957 and 2002. Furthermore, Gower (2002) used buoy data and found that WS and SWH in the northeast Pacific had increased by about 10–50 cm s^{-1} decade^{-1} and 10–40 cm decade^{-1} for the period 1977–1999, respectively.

In this current study, long-term trends in sea surface WS and SWH between 1988 and 2011 are presented for the China Seas using CCMP ocean surface wind data and 24-year hindcast wave dataset obtained from the WW3 wave model forced with CCMP ocean surface winds. An assessment of regional differences is also included in the analysis. Located at the edge of western Pacific Ocean, the China Seas are significantly influenced by the monsoon, and it is thus expected that results will show that long-term trends in WS and SWH in the region are closely related to monsoon variability, in addition to atmospheric circulation and wider global climate changes. The authors acknowledge that a few previous studies have focused on these trends within the same region.

2 Data and Methodology

2.1 Methodology

The WW3 wave model driven by CCMP ocean surface winds is used to simulate the three-hourly wave field for the China Seas from 0000 UTC on 1 January 1988 to 1800 UTC on 31 December 2011. The precision of these simulated data was verified using wave statistics data obtained from Korean and Japanese buoys. Finally, 24-yr trends in WS and SWH are calculated across the China Seas using CCMP winds and simulated wave data, and the long-term trends in regional and seasonal differences are assessed.

To improve validity of the simulated wave data in this study, the region of interest was extended and nested (Fig.1). The parent domain was set as the northwestern Pacific (5.125˚S–45.125˚N, 90.125˚–180.125˚E) and the nested domain comprises the China Seas and surrounding waters (0˚–41˚N, 100˚–130˚E). The spatial resolution of the model output was 0.25˚×0.25˚, the time step used was 900 s, and the output interval 3 hours.

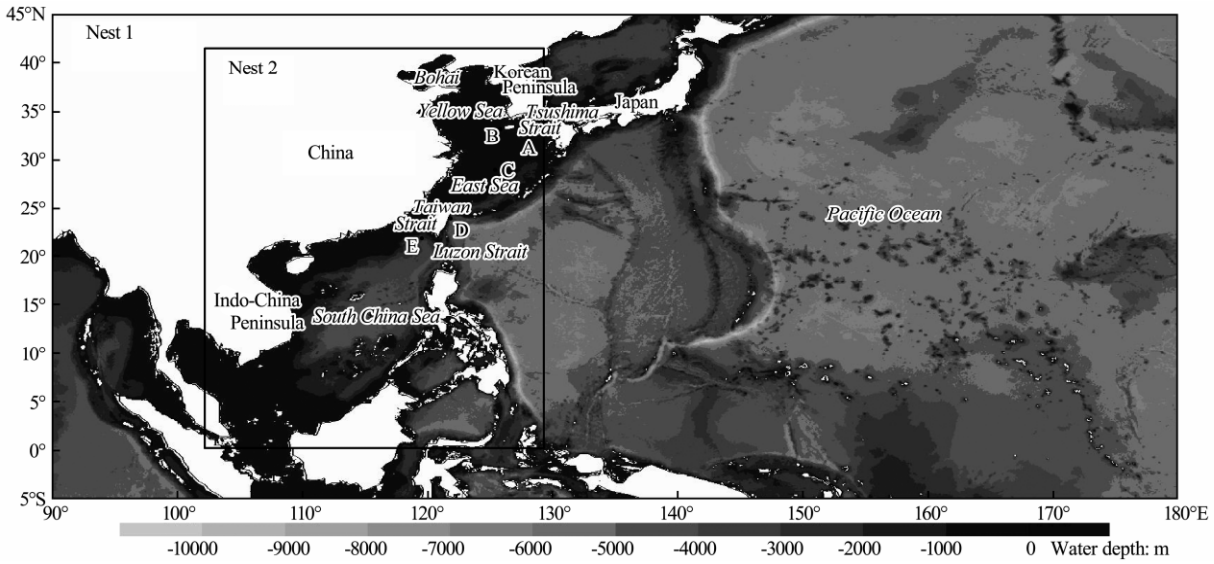

Fig.1 Topography of China seas, and buoy locations. A, Fukue Island station; B, Cheju Island station; C, station 22001; D, Hualian station; E, Dongsha station.

2.2 Wind Field Data

The CCMP ocean surface wind product is distributed by the Physical Oceanography Distributed Active Archive Center (PO.DAAC) and has been evaluated and used extensively by the scientific community (Atlas *et al*., 2011). These data are derived through cross-calibration and assimilation of ocean surface wind data from the Special Sensor Microwave Imager (SSM/I), Tropical Precipitation Measurement Mission (TRMM)-Microwave Imager (TMI), Advanced Microwave Scanning Radiometer-Earth Observing System (AMSR-E), SeaWinds on QuikSCAT, and SeaWinds on ADEOS-II. Cross calibration is performed by Remote Sensing Systems (RSS) under the DISCOVER project. These datasets are combined with conventional observations and a starting estimate of the

?1994-2017 China Academic Journal Electronic Publishing House. All rights reserved. http://www.cnki.net

wind field using the variational analysis method (VAM), which requires a background (or first guess) analysis of gridded *u* and *v* wind components as a prior estimate of the wind field (Zheng and Pan, 2014; Zheng and Li, 2015). The 40-year European Centre for Medium-Range Weather Forecasting (ECMWF) Re-Analysis (ERA-40) is used as the background for the period July 1987 to December 1998. ECMWF operational (ECOP) analysis has the advantage of four-dimensional variational data assimilation (4DVAR) and increased spatial resolution; it thus outperforms ERA-40 and is used in this study for the background starting from 1999. The temporal resolution of the CCMP product is 6 h. It covers the period July 1987 to July 2011, has a spatial resolution of 0.25°×0.25°, and spans are region from 78.375°S–78.375°N and 0.125°–379.875°E. Carvalho *et al*. (2013) found that CCMP enables substantial improvements in terms of wind direction temporal variability and wind speed mean state compared with ocean surface wind data derived from several QuikSCAT products. In addition, Carvalho *et al.* (2015) compared offshore wind data derived from satellite measurements (CCMP, QuikSCAT, National Climatic Data Center (NCDC) Blended Sea Winds, and French Research Institute for Exploitation of the Sea (IFREMER) Blended Wind Fields) with in situ measurements, and found that CCMP winds have the lowest error for mean wind speed estimation.

2.3 Data Validation

The precision of simulated wave data was validated using hourly measurements from Japanese, Korean, and Taiwanese buoys (locations shown in Fig.1). A quantile-quantile comparison (from the 1st to 99th percentiles) between simulated and observed SWH was correlated (Fig.2) and results were found to be in generally good agreement for each station (Fukue Island, Cheju Island, station 22001, Dongsha Island, and Hualian Island); however, simulated SWH was underestimated for Hualian Island in October 2011 (Fig.2h).

To quantitatively analyze the accuracy of simulated SWH, the precision of simulated wave data was calculated following Rascle and Ardhuin (2013). The correlation coefficient (CC), bias, root mean square error (RMSE), and normalized root mean square error (NRMSE) are shown in Table 1. Regardless of differences in site and season, simulated and observed SWH are highly correlated (CC larger than 0.90 and significant at the 99% level), and the error in the simulated data remains low according to RMSE and MAE values. SWH estimates

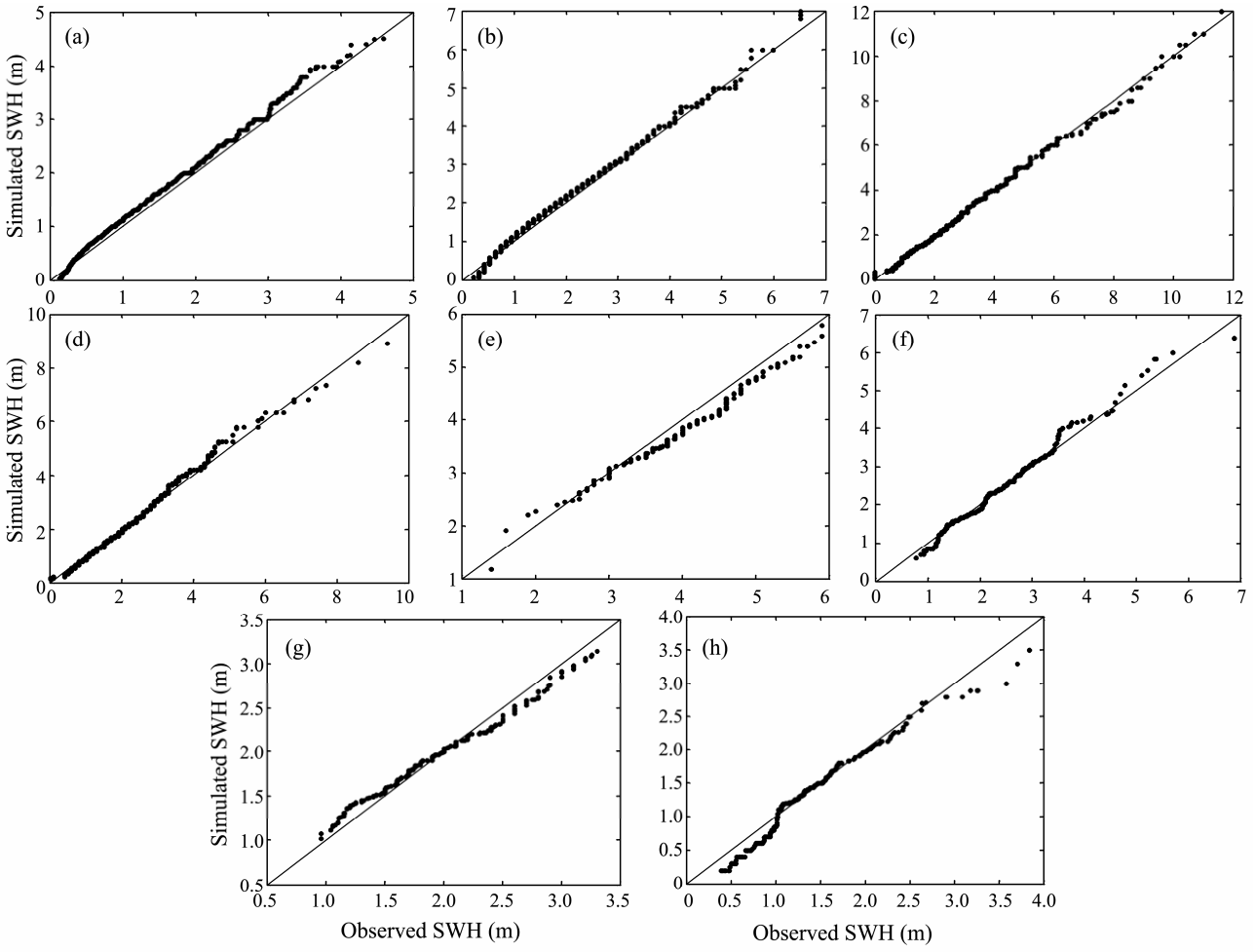

Fig.2 Quantile-quantile comparison of simulated SWH and observed SWH for: (a) Fukue Island in 2009, (b) Cheju Island in 2010, (c) Station 22001 in 1996, (d) Station 22001 in 1998, (e) Dongsha Island in January 2011, (f) Dongsha Island in October 2011, (g) Hualian Island in January 2011, and (h) Hualian Island in October 2011.

?1994-2017 China Academic Journal Electronic Publishing House. All rights reserved. http://www.cnki.net

Table 1 Precision of simulated significant wave height estimates

Station	Location		Time	CC	Bias	RMSE	NRMSE
	Longitude (˚E)	Latitude (˚N)					
Fukue Island	128.63	32.76	2009	0.86	–0.11	0.36	0.15
Cheju Island	126.03	33.08	2010	0.89	–0.16	0.40	0.13
22001	126.33	28.17	1996	0.94	0.01	0.45	0.14
			1998	0.92	0.13	0.40	0.11
Hualian	121.63	24.04	Jan 2011	0.90	0.06	0.24	0.12
			Oct 2011	0.96	0.02	0.20	0.10
Dongsha	118.83	21.04	Jan 2011	0.90	0.19	0.39	0.09
			Oct 2011	0.96	0.01	0.27	0.10

from buoy observations and satellite data inversion have been used in previous studies to validate simulated SWH and results show that simulated data are highly reliable (Zheng *et al*., 2016a; Zheng *et al*., 2014). The ability of WW3 to successfully simulate the wave field in the China Seas has also been demonstrated in previous studies (Chu *et al*., 2004; Mirzaei *et al*., 2013). Based on the evidence presented in this study, it can be concluded that simulated SWH is reliable in the China Seas.

3 Long-Term Trends in SWH and WS

3.1 Area-Averaged SWH and WS Trends

The average annual WS value in 1988 was calculated for each 0.25˚×0.25˚ cell in the China Seas (0˚−41˚N, 100˚−130˚E). A zonal average value of WS was then obtained using the Thiessen polygon method, and this method was also used to obtain 24 zonal and yearly average WS values. Finally, the overall variation of the WS in the China Seas was analyzed (as shown in Fig.3a) and the overall variation in SWH in the China Seas was also analyzed (as shown in Fig.3b). Results show that the correlation coefficient (R) of WS is 0.82 (significant at a 99% reliability level) and the increasing trend is significant (with a regression coefficient of 0.0338). Therefore, WS in the China Seas exhibited a significant increasing trend of 3.38 cm s^{-1} yr^{-1} over the period 1988–2011. Similarly, SWH in the China Seas (Fig.3b) showed a significant increasing trend of 1.3 cm yr^{-1} over the 24-yr period.

Zheng *et al.* (2016b) found a significant increasing trend in WS over most of the global ocean; this trend was 3–11 cm s^{-1} yr^{-1} for the China Seas. Using a 23-year database of calibrated and validated satellite altimeter measurements, Young *et al.* (2011) found a significant increasing trend in SWH for most of the global ocean, and a rate of 2.64–4.50 cm yr^{-1} in the China Seas. It is apparent that the values from the analysis conducted in this study with respect to the China Seas are slightly smaller than those obtained by Young *et al*. (2011) and Zheng *et al.* (2016b). However, comparing the results presented here with those of Zieger *et al*. (2014), who found a significant increasing global average trend in WS (0.203 m s^{-1} decade^{-1} using altimeter data, and 0.093 m s^{-1} decade^{-1} using data from SSM/I) for the period 1991–2008, it can be concluded that the increasing trend in WS over the China Seas is slightly larger than that of the global average trend.

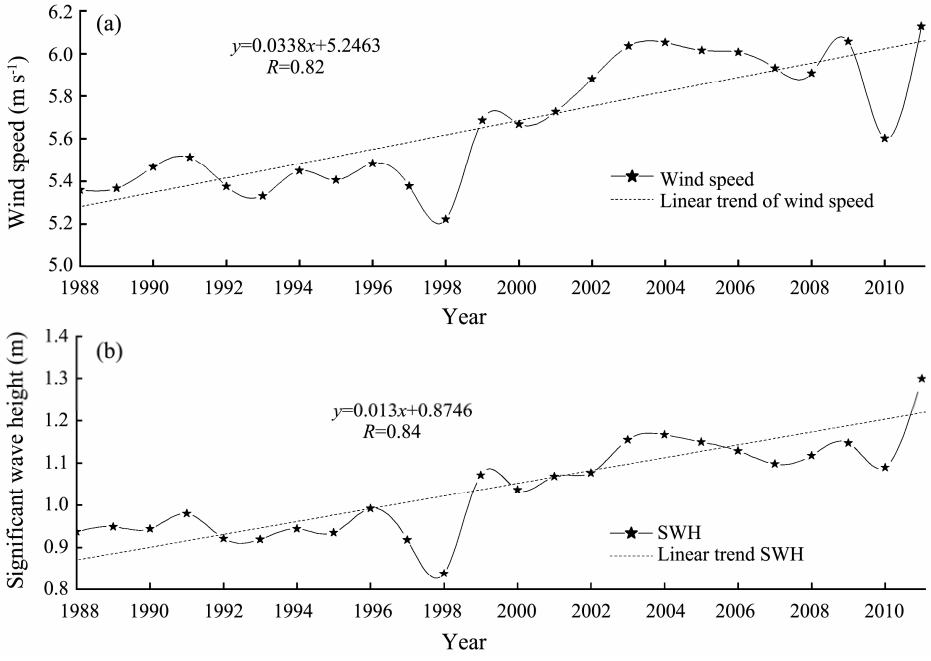

Fig.3 Long-term trends in area-averaged (a) surface wind speed and (b) significant wave height for China Seas.

?1994-2017 China Academic Journal Electronic Publishing House. All rights reserved. http://www.cnki.net

3.2 Regional Differences in Long-Term Trends of SWH and WS

To explore regional differences in trends of SWH and WS, the long-term trends for the period 1988–2011 were calculated for each 0.25°×0.25° region in the China Seas and results show notable regional differences (Fig.4). For example, WS over most waters north of 17°N exhibits a significant increasing trend, areas without significant changes are located mainly in the middle of the middle-low latitude areas in the South China Sea (SCS), areas exhibiting a decreasing trend are distributed sporadically, and areas with a relatively strong increasing trend are located mainly in the middle of the Bohai Sea (about 9 cm $s^{-1} yr^{-1}$), the Tsushima Strait (12–15 cm $s^{-1} yr^{-1}$), the northern (about 9 cm $s^{-1} yr^{-1}$) and southern zones of the Taiwan Strait (12–15 cm $s^{-1} yr^{-1)}$, and nearshore in the northern SCS (6–9 cm $s^{-1} yr^{-1}$). Our calculated rate of WS increase over the China Seas is close to the value (3–11 cm $s^{-1} yr^{-1}$) obtained by Zheng *et al*. (2016b).

Between 1988 and 2011, most regions of the China Seas experienced a significant increasing trend in SWH of > 1.5 cm yr^{-1}. Areas with a strong increasing trend are primarily located in the Tsushima Strait (> 3.0 cm yr^{-1}), waters near the Ryukyu Islands (2.5–3.5 cm yr^{-1}), the Taiwan Strait (> 2.5 cm yr^{-1}), and waters north of 15°N in the SCS (> 3.0 cm yr^{-1}), particularly southwest of Taiwan Strait (> 4.0 cm yr^{-1}). It is of note that these values are slightly lower than the values obtained by Young *et al.* (2011).

A comparison between Figs.4a and 4b shows that the long-term trend in SWH was consistent with that of the WS over the 24 years studied, particularly in regions with a strong increasing trend. These findings can be explained by the fact that the China Seas are classified as marginal seas, where the wave field is primarily controlled by the local wind field rather than swell (Semedo *et al*., 2011).

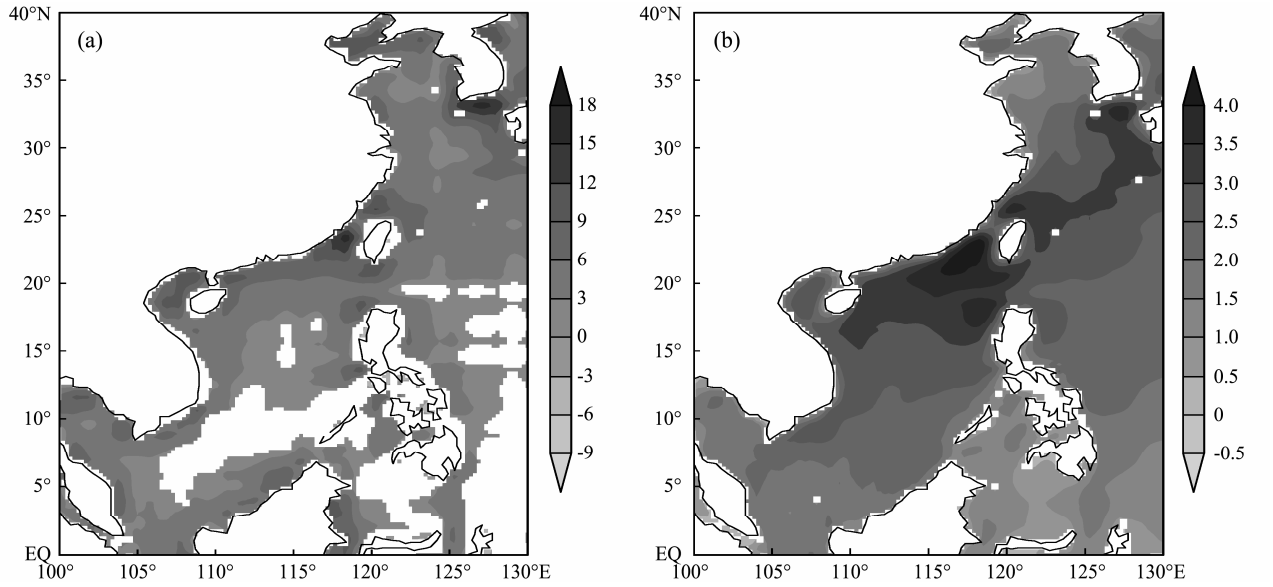

Fig.4 Long-term trends in: (a) WS (cm $s^{-1} yr^{-1}$) and (b) SWH (cm yr^{-1}) over the period 1988–2011 in the China Seas (only trends significant at the 95% level are shown).

The trends in WS and SWH in this study are similar to the results reported by Young *et al*. (2011) for the China Seas (10.04–13.76 cm $s^{-1} yr^{-1}$ in the WS, and 2.64–4.50 cm yr^{-1} in SWH, although the rate of increase in WS is slightly larger than the value of 4 cm $s^{-1} yr^{-1}$ reported by Thomas *et al.* (2008). However, the increasing trend in SWH is slightly larger than the result reported by Semedo *et al*. (2011) for the China Seas (0.5–1.5 cm yr^{-1}).

Using deep-water wave buoy data offshore from the U.S. Pacific Northwest, Ruggiero *et al.* (2010) found an increasing trend in annual average SWH of about 1.50 cm yr^{-1} since the mid-1970s. Therefore, the increase in SWH in the China Seas is larger than the increase for offshore region of the U.S. Pacific Northwest. Wang and Swail (2001) reported that SWH in the North Pacific and North Atlantic exhibited a significant increasing trend over the previous four decades, and that multidecadal fluctuations were significant (especially in the North Pacific); the result presented in this study is close to the value reported. Mori *et al.* (2010) predicted the future ocean wave climate and compared it with present conditions. Using an atmospheric general circulation model coupled to a global wave model, they reported that future wave heights will increase at middle latitudes and in the Antarctic Ocean, but will decrease at the equator. This study presents the climatic trends of WS and SWH for the past 24 years. In the future work, it is also needed to analyze the future trend of WS and SWH in the China Seas, referring to the method provided by Mori *et al.* (2010). Combing the trends of WS and SWH for both the past and future will provide a more scientific reference for the related research and engineering.

4 Discussion

The occurrence of both gales (WS > 10.8 m s^{-1}) and

?1994-2017 China Academic Journal Electronic Publishing House. All rights reserved. http://www.cnki.net

rough seas (SWH > 2.5 m) increased significantly between 1988 and 2011 (Fig.5).

A comparison between Fig.4a and 5a shows that long-term trends in wind speed and gale occurrence have similar spatial distributions. It is thus considered that the increasing trend in gale occurrence is the main reason for the increase in WS over the China Seas. Gale occurrence shows a significant year-on-year linear increase over large-scale sea areas north of 18˚N, in the Beibu Gulf, and in areas surrounding the Indochina peninsula (Fig.5a). The Taiwan Strait and Tsushima Strait show the strongest increasing trend, with values above 0.6% yr^{-1} and above 1.0% yr^{-1}, respectively (where % is gale occurrence, not variability of gale occurrence).

The long-term trend in rough sea occurrence (expressed as % yr^{-1}, where % is rough sea occurrence, not variability of rough sea occurrence) is presented in Fig.5b. It is evident that the long-term characteristics of the rough sea occurrence distribution are similar to those for gale occurrence, and it is considered that this is related to the dominant role of the wind sea.

The possible reasons for wind speed variations include: 1) variation in atmospheric circulation and the monsoon system, 2) substrate differences and urbanization, or 3) a combination of both 1) and 3). Studies by Young *et al.* (2011), Gulev and Grogorieva (2004), Gulev and Hasse (1999), Ranasinghe *et al.* (2004), and Bertin *et al.* (2013) have provided evidence for the long-term increase in SWH when superimposed on interannual variability controlled by oscillating phenomena, such as the NAO in the North Atlantic Ocean or El Niño in the Pacific Ocean.

Applying their methods to the China Seas shows a connection between rough sea occurrence (and gale occurrence) and El Niño between 1988 and 2011 (Fig.6).

However, in the China Seas and surrounding waters, rough sea occurrence and the contemporaneous Niño3 index show a significant negative correlation; this is also true for a 1–4 month delayed rough sea occurrence. This negative correlation is strongest (and the area is most significant at the 95% level) using a two-month delayed rough sea occurrence. The strongest negative correlation ($R = -0.6$) is found for waters surrounding Taiwan, the northern SCS, and waters to the east of the Philippines, and is also significant in central areas of the Yellow Sea ($R = -0.5$). However, when the rough sea occurrence is delayed for five months, the correlation becomes weaker and the significant negative correlation is limited only to isolated sea areas. The relationship between gale occurrence and Niño3 index (Figures omitted) is similar to the relationship between rough sea occurrence and Niño3 index. Here, we also calculated the periods of gale occurrence and Niño3 index for the period 1988–2011 separately using wavelet analysis (Figures omitted). Gale occurrence shows the same variation period of about three years with Niño3. The Niño3 shift of July 1999 and November 2000 is about half a year ahead of the gale occurrence shift in the China Seas. It is considered that the sea surface temperature shift in the Niño3 area may be the main driving factor behind the gale occurrence shift over the China Seas. In this respect, Gulev and Grigorieva (2004) showed that WS variation over the Pacific and changes to wind wave heights in the region are closely related to the El Niño-Southern Oscillation (ENSO). Unlike the land surface wind speed, the long-term trend of wind speed in the China Seas is affected little by substrate differences, urbanization, or other human factors. We therefore conclude that gale occurrence over the China Seas and surrounding waters is closely related to variations in sea surface temperature within the Niño3 region, which means that El Niño has a significant influence on gale occurrence in the region.

The China Seas are often subjected to cold air with a northerly or northeasterly prevailing wind direction. In addition, there is a decrease in wind speed during the

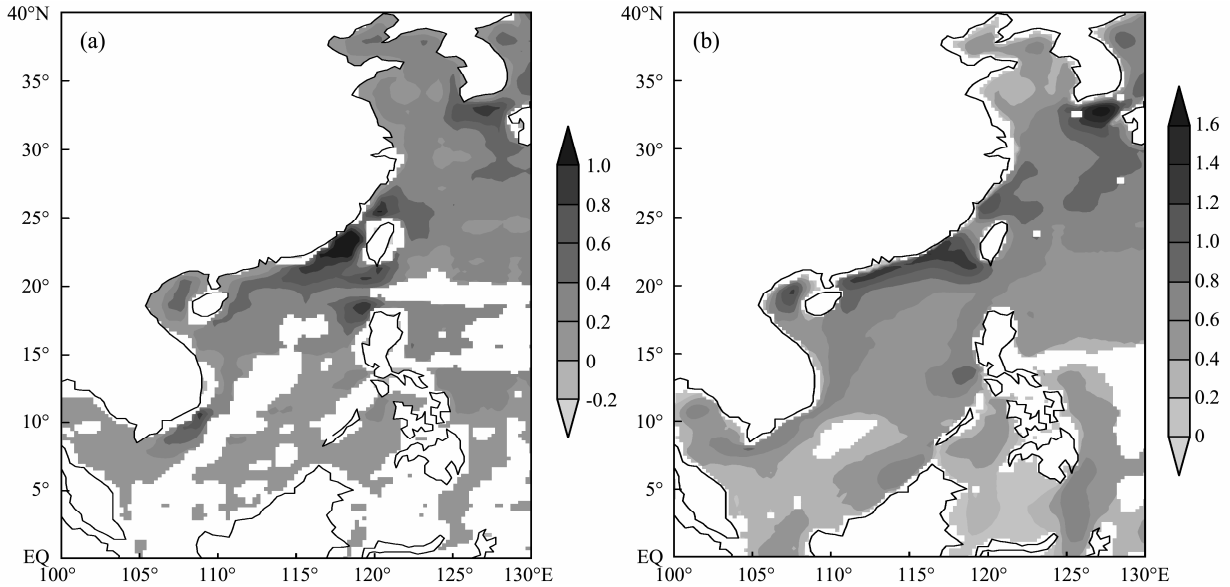

Fig.5 Long-term trend in: (a) gale occurrence (% yr^{-1}) and (b) rough sea occurrence (% yr^{-1}) (only trends significant at the 95% level are shown).

?1994-2017 China Academic Journal Electronic Publishing House. All rights reserved. http://www.cnki.net

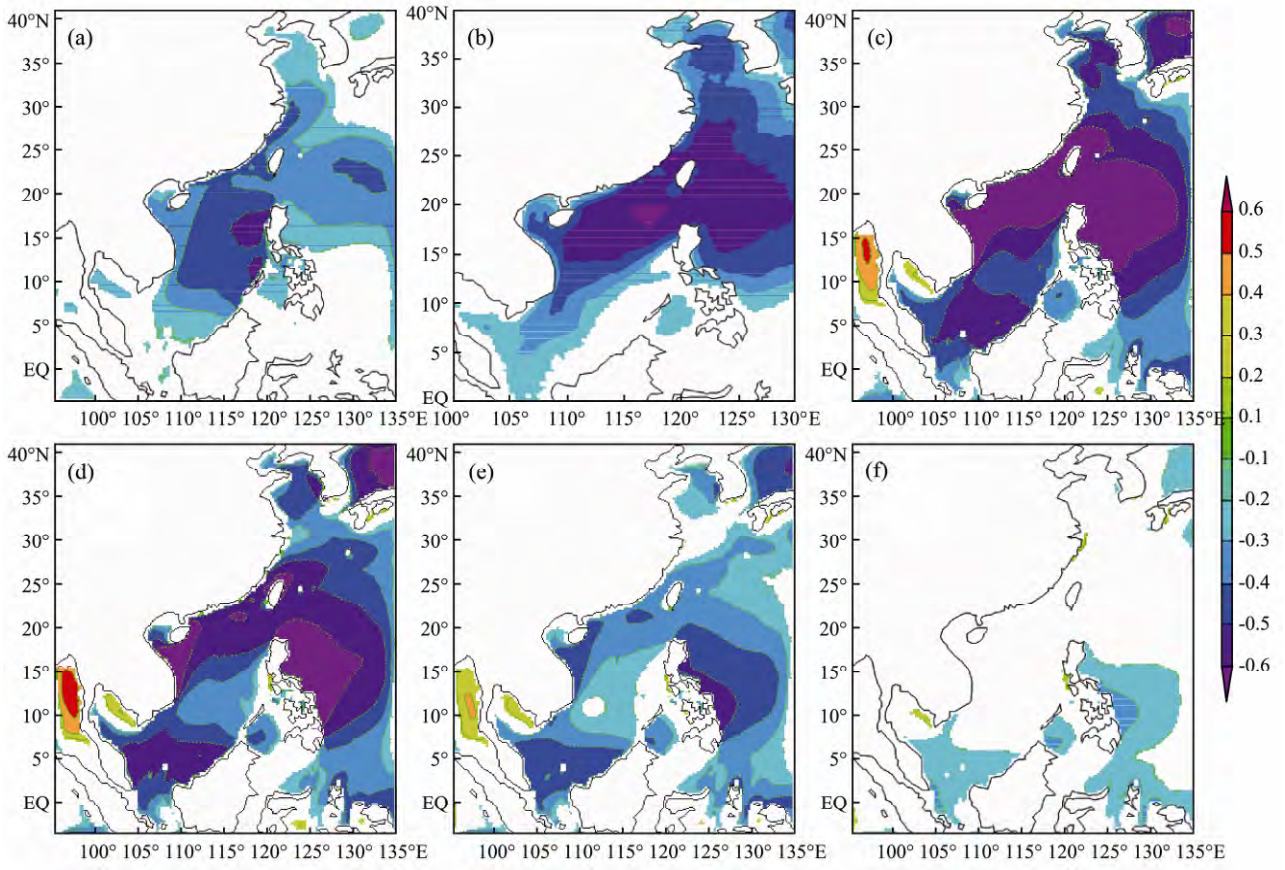

Fig.6 Relationship between rough sea occurrence and Niño3 index for China Seas and surrounding waters: (a) contemporaneous correlation, (b–f) correlation between Niño3 index and 1–5 month delayed rough sea occurrence (only areas significant at the 95% level are shown).

transition season of the monsoon. The studies by Li (1990) and Chen *et al*. (2000) have shown that interannual variability in the East Asian monsoon is correlated with ENSO. The East Asian monsoon is always relatively weak during El Niño years and relatively strong during La Niña years, and this could account for the significant negative correlation between gale occurrence over the China Seas and the Niño3 index for the corresponding period. Mirzaei *et al*. (2013) found that SWH in the SCS correlated negatively with Niño3.4 index during winter, spring, and autumn, but became positive in the summer monsoon, and such correlations correspond well with the surface wind anomalies over the SCS during El Niño events. We thus further conclude that the increasing trend in WS over the China Seas is driven mainly by atmospheric circulation, monsoon variations, and ENSO.

After calculating the area-average rough sea occurrence in the China Seas, we compared the rough sea occurrence with trends in monthly variations of the Niño3 index and found that the negative correlation between rough sea occurrence and Niño3 index was greatest when rough sea occurrence was delayed by two months ($R = -0.61$, significant at the 99.9% level; Fig.7); the reverse trend between the two curves is clear.

The occurrence of an unusual phenomenon was also determined in 1998, which could be related to an abrupt period. Zhou *et al*. (2009) reported highly unusual air and ground temperatures associated with the intense ENSO event of 1998. Zhou and Wen (2007) found the abnormality of precipitation in 1998, which is an important characteristic of the monsoon. These studies show that there were abnormalities in the East Asia monsoon in around 1998. The China Seas are located at the edge of the ocean (also the East Asia monsoon zone), and consequently the influence of wind seas in the mixed seas is relatively high. Accordingly, East Asia monsoon abnormalities may lead to wave field abnormalities in the China Seas. The abnormalities shown in Fig.7 are thus consistent with the conclusions of Zhou *et al*. (2009), and Zhou and Wen (2007).

In summer, the China Seas are affected by the southwest monsoon with a southerly to southwesterly prevailing wind direction. Generally, the wind speed in the monsoon transition season is relatively low. For example, in El Niño (La Niña) years, the average Hadley circulation and Ferrel circulation strengthens (weakens). In addition, significant southern (northern) wind abnormalities and northward (southward) thermal conveyance abnormalities exist in the zone between 30˚N and 60˚N. Midlatitude zonal westerlies also strengthen (weaken). All of these effects may enhance (restrict) the southward outburst of cold air (Zhai *et al*., 2001). Simultaneously, the existence of a negative sea surface temperature anomaly in the tropical western Pacific leads to the formation of anticyclonic (cyclonic) circulation, which may then weaken (strengthen) the winter monsoon (Zhang *et al*.,

?1994-2017 China Academic Journal Electronic Publishing House. All rights reserved. http://www.cnki.net

1996; Wang *et al*., 2000). In summary, winter gust occurrence over the China Seas may weaken (strengthen) in El Niño (La Niña) years. Wang (2001) indicated that El Niño (La Niña) induces a weakening (strengthening) effect on the East Asia summer monsoon; the strengthening effect is found mainly to the south of the Yangtze River. Our results also reveal that both gust occurrence and billow frequency exhibit a significant negative correlation with the Niño3 index, and these results are consistent with the findings of Li (1990), Zhai *et al*. (2001) and Wang (2001).

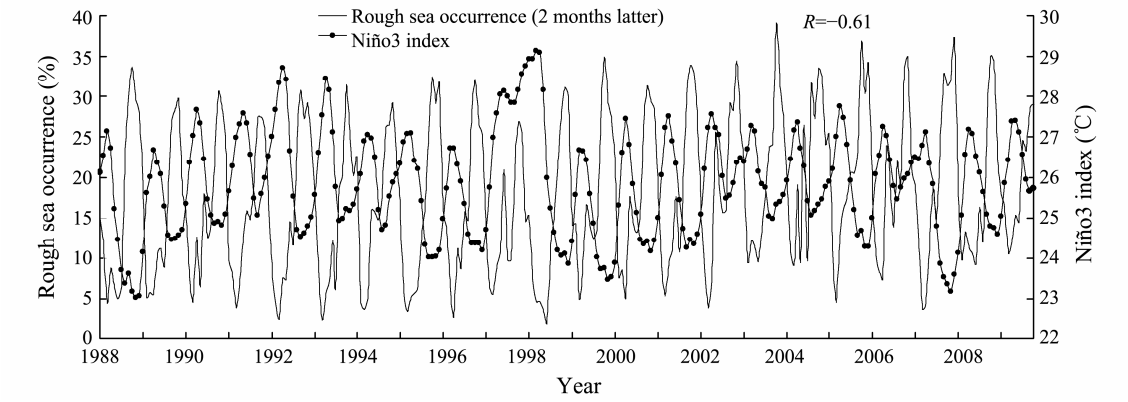

Fig.7 Relationship between Niño3 index and two-month delayed regional average for rough sea occurrence.

5 Conclusions

This paper presents the long-term trends in surface wind speed and significant wave height for the China Seas during the period 1988–2011. These trends are derived from the CCMP ocean surface wind data together with a 24-year hindcast wave dataset obtained using the WW3 wave model forced with CCMP wind fields. The results may be summarized as follows.

1) For the period 1988–2011, there was a significant increasing trend in WS (3.38 cm s^{-1} yr^{-1}) and SWH (1.52 cm yr^{-1}) in the China Seas.

2) Over the 24-year study period, there were regional differences in the long-term trends of SWH and WS. Wind speed over most of the China Seas showed a significant yearly linear increasing trend, and areas without significant long-term trends were located mainly in the middle of the middle–low latitude regions of the SCS and in waters to the east of the Philippines; however, a few isolated regions showed a decreasing trend. Areas with a strong increasing trend were located mainly in the middle of the Bohai Sea, the Tsushima Strait, northern and southern areas of the Taiwan Strait, and the nearshore zone of the northern SCS. Between 1988 and 2011, most regions in the China Seas showed a significant increasing trend in SWH of above 1.5 cm yr^{-1}. Areas with a strong increasing trend were located primarily in the Tsushima Strait (> 3.0 cm yr^{-1}), waters near the Ryukyu Islands (2.5–3.5 cm yr^{-1}), the Taiwan Strait (> 2.5 cm yr^{-1}), large areas to the north of 15˚N in the SCS (> 3.0 cm yr^{-1}), and southwest of the Taiwan Strait (> 4.0 cm yr^{-1}).

3) The long-term trend in WS over the China Seas was closely associated with both the El Niño phenomenon and the significant increasing trend in gale occurrence over the 24-year period. Gale occurrence, with the wind level above 6 on the Beaufort Scale, shows a significant increasing trend for regions north of 18˚N, the Beibu Gulf, and waters surrounding the Indochina peninsula. The Taiwan Strait and the Tsushima Strait showed the strongest increasing trend, with values above 0.6 % yr^{-1} and above 1.0 % yr^{-1}, respectively. Over the China Seas and surrounding waters, gale occurrence and the contemporaneous Niño3 index were significantly negatively correlated; this was also true for a 1–4 month delayed gale occurrence. The negative correlation was strongest, and the area significant at the 95% level was largest, when gale occurrence was delayed by two months.

Acknowledgements

We thank the anonymous reviewers and the editor for their constructive comments that helped to improve this paper. This work was supported by the Global Change and Ocean-Atmosphere Interaction National Special Project (No. 2016-523), the open foundation of the Key Laboratory of Renewable Energy, Chinese Academy of Sciences (No. Y707k31001), the Junior Fellowships for CAST Advanced Innovation Think-Tank Program (No. DXB-ZKQN- 2016-019), the National Key Basic Research Development Program (No. 2012CB957803), the National Natural Science Foundation of China (Nos. 41490642, 41405062, 71371148), the Fundamental Research Funds for the Central Universities (No. 3132017301), and the Science found- ation of China (Xi'an) Silk Road Academy (No. 2016SY02).

References

Amiri, A., Panahi, R., and Radfar, S., 2016. Parametric study of two-body floating-point wave absorber. *Journal of Marine Science and Application*, **15** (1): 41-49.

Atlas, R., Hoffman, R. N., Ardizzone, J., Leidner, S. M., Jusem, J. C., Smith, D. K., and Gombos, D., 2011. A cross-calibrated, multiplatform ocean surface wind velocity product for meteorological and oceanographic applications. *American Meteorological Society*, **92**: 157-174.

Behzad, H., and Panahi, R., 2017. Optimization of bottom-

?1994-2017 China Academic Journal Electronic Publishing House. All rights reserved. http://www.cnki.net

hinged flap-type wave energy converter for a specific wave rose. *Journal of Marine Science and Application*, **16** (2): 159-165.

Bertin, X., Prouteau, E., and Letetrel, C., 2013. A significant increase in wave height in the North Atlantic Ocean over the 20th century. *Global and Planetary Change*, **106**: 77-83.

Carniello, L., Alpaos, A. D., and Defina, A., 2011. Modeling wind waves and tidal flows in shallow micro-tidal basins. *Estuarine, Coastal and Shelf Science*, **92** (2): 263-276.

Carvalho, D., Rocha, A., Gómez-Gesteira, M., Alvarez, I., and Santos, C. S., 2013. Comparison between CCMP, QuikSCAT and buoy winds along the Iberian Peninsula coast. *Remote Sensing of Environment*, **137**: 173-183.

Carvalho, D., Rocha, A., Gómez-Gesteira, M., and Santos, C. S., 2015. Comparison of reanalyzed, analyzed, satellite-retrieved and NWP modelled winds with buoy data along the Iberian Peninsula coast. *Remote Sensing of Environment*, **152**: 480-492.

Chen, W., Hans, F. G., and Huang, R. H., 2000. The interannual variability of East Asian winter monsoon and its relation to the summer monsoon. *Advances in Atmospheric Sciences*, **17**: 46-60.

Chu, P. C., Qi, Y. Q., Chen, Y. C., Shi, P., and Mao, Q. W., 2004. South China Sea wind-wave characteristics. Part I: Validation of wavewatch-III using TOPEX/Poseidon data. *Journal of Atmospheric and Oceanic Technology*, **21**: 1718-1733.

Church, J., and White, N., 2006. A 20th century acceleration in global sea-level rise. *Geophysical Research Letters*, **33** (1): L01602, DOI: 10.1029/2005GL024826.

Das, S., and Crepin, A. S., 2013. Mangroves can provide protection against wind damage during storms. *Estuarine, Coastal and Shelf Science*, **134**: 98-107.

Dodet, G., Bertin, X., and Taborda, R., 2010. Wave climate variability in the North-East Atlantic Ocean over the last six decades. *Ocean Modeling*, **31** (3-4): 120-131.

Gower, J. F. R., 2002. Temperature, wind and wave climatologies, and trends from marine meteorological buoys in the northeast pacific. *Journal of Climate*, **15**: 3709-3718.

Gulev, S. K., and Grigorieva, V., 2004. Last century changes in ocean wind wave height from global visual wave data. *Geophysical Research Letters*, **31**: L24302, DOI: 10.1029/2004GL021040.

Gulev, S. K., and Grigotieva, V., 2006. Variability of the winter wind waves and swell in the North Atlantic and North Pacific as revealed by the voluntary observing ship data. *Journal of Climate*, **19**: 5667-5685.

Gulev, S. K., and Hasse, L., 1999. Changes of wind waves in the north Atlantic over the last 30 years. *International Journal of Climatology*, **19**: 1091-1117.

IPCC (Intergovernmental Panel on Climate Change), 2013. *Climate Change 2013: The Physical Science Basis. Contribution of Working Group I to the Fourth Assessment Report of the Intergovernmental Panel on Climate Change*. Stocker, T. F., *et al.*, eds., Cambridge University Press, Cambridge, 5pp.

Li, C. Y., 1990. Interaction between anomalous winter monsoon in East Asia and El Niño events. *Advances in Atmospheric Sciences*, **7** (1): 36-46.

Li, X., and Dong, S., 2016. A preliminary study on the intensity of cold wave storm surges of Laizhou Bay. *Journal of Ocean University of China*, **15** (6): 987-995.

Mei, Y., Song, S., and Zhou, L., 2010. Annual variation characteristics of wave fields and wind fields over the North Indian Ocean and South China Sea. *Marine Forecasts*, **27** (5): 27-33 (in Chinese with English abstract).

Mirab, H., Fathi, R., Jahangiri, V., Ettefagh, M., and Hassannejad, R., 2015. Energy harvesting from sea waves with consideration of airy and JONSWAP theory and optimization of energy harvester parameters. *Journal of Marine Science and Application*, **4**: 440-449.

Mirzaei, A., Tangang, F., Juneng, L., Mustapha, M. A., Husain, M. L., and Akhir, M. F., 2013. Wave climate simulation for southern region of the South China Sea. *Ocean Dynamics*, **63 (8)**: 961-977.

Mohapatra, S., 2016. The interaction of oblique flexural gravity waves with a small bottom deformation on a porous oceanbed: Green's function approach. *Journal of Marine Science and Application*, **2**: 112-122.

Mori, N., Yasuda, T., Mase, H., Tom, T., and Oku, Y., 2010. Projection of extreme wave climate change under global warming. *Hydrological Research Letters*, **4**: 15-19.

Ranasinghe, R., McLoughlin, R., Short, A., and Symonds, G., 2004. The Southern Oscillation Index, wave climate, and beach rotation. *Marine Geology*, **204** (3): 273-287.

Rascle, N., and Ardhuin, F., 2013. A global wave parameter database for geophysical applications. Part 2: Model validation with improved source term parameterization. *Ocean Modelling*, **70**: 174-188.

Reza, T. M., Mani, F. D., and Ali, D. D. M., 2017. Response spectrum method for extreme wave loading with higher order components of drag force. *Journal of Marine Science and Application*, **16** (1): 27-32.

Ruggiero, P., Komar, P. D., and Allan, J. C., 2010. Increasing wave heights and extreme value projections: The wave climate of the U.S. Pacific Northwest. *Coastal Engineering*, **57**: 539-552.

Semedo, A., Suselj, K., Rutgersson, A., and Sterl, A., 2011. A global view on the wind sea and swell climate and variability from ERA-40. *Journal of Climate*, **24**: 1461-1479.

Sun, L., Yu, H. M., and Wang, P., 2010. Analysis of the seasonal and interannual variability of sea surface wind in the East China Seas and its adjacent ocean. *Marine Forecasts*, **27** (2): 30-37 (in Chinese with English abstract).

Thomas, B. R., Kent, E. C., Swail, V. R., and Berry, D. I., 2008. Trends in ship wind speeds adjusted for observation method and height. *International Journal of Climatology*, **28**: 747-763.

Wang, B., Wu, R. G., and Fu, X. H., 2000. Pacific-East Asian teleconnection: How does ENSO affect East Asian climate? *Journal of Climate*, **13**: 1517-1536.

Wang, S. W., 2001. *Advance in Climate Research*. China Meteorological Press, Beijing, 165-168.

Wang, X. L., and Swail, V. R., 2001. Changes of extreme wave heights in northern Hemisphere oceans and related atmospheric circulation regimes. *Journal of Climate*, **14** (10): 2204-2221.

Ward, M. N., and Hoskins, B., 1996. Near surface wind over the global ocean 1949–1988. *Journal of Climate*, **9**: 1877-1895.

Young, I. R., Zieger, S., and Babanin, A. V., 2011. Global trends in wind speed and wave height. *Science*, **332** (6028): 451-455.

Zhai, P. M., Guo, Y. J., and Li, X. Y., 2001. A diagnostics analysis of 1997/1998 ENSO event and role of intra-seasonal oscillation in the tropical atmosphere. *Journal of Tropical Meteorology*, **7** (2): 113-121.

Zhang, R. H., Sumi, A., and Kinoto, M., 1996. Impact of El Niño on the East Asian monsoon: A diagnostic study of the '86/87' and '91/92' events. *Journal of the Meteorological Society of Japan*, **74**: 49-62.

Zheng, C. W., and Li, C. Y., 2015. Variation of the wave energy and significant wave height in the China Sea and adjacent

?1994-2017 China Academic Journal Electronic Publishing House. All rights reserved. http://www.cnki.net

waters. *Renewable and Sustainable Energy Reviews*, **43**: 381-387.

Zheng, C. W., and Li, C. Y., 2017. Propagation characteristic and intraseasonal oscillation of the swell energy of the Indian Ocean. *Applied Energy*, **197**: 342-353.

Zheng, C. W., and Pan, J., 2014. Assessment of the global ocean wind energy resource. *Renewable and Sustainable Energy Reviews*, **33**: 382-391.

Zheng, C. W., Li, C. Y., Yang, Y., and Chen, X., 2016a. Analysis of wind energy resource in the Pakistan's Gwadar Port. *Journal of Xiamen University (Natural Science Edition)*, **55** (2): 210-215 (in Chinese with English abstract).

Zheng, C. W., Pan, J., and Li, C. Y., 2016b. Global oceanic wind speed trends. *Ocean & Coastal Management*, **129**: 15-24.

Zheng, C. W., Shao, L. T., Lin, G., and Pan, J., 2014. Analysis of influence on the security of sea skimming caused by a typhoon wave. *Journal of Harbin Engineering University*, **35** (3): 301-306 (in Chinese with English abstract).

Zheng, C. W., Wang, Q., and Li, C. Y., 2017. An overview of medium- to long-term predictions of global wave energy resources. *Renewable and Sustainable Energy Reviews*, **79C**: 1492-1502.

Zheng, C. W., Zhou, L., Shi, W. L., Li, X., and Huang, C. F., 2015. Decadal variability of global ocean significant wave height. *Journal of Ocean University of China*, **14** (5): 778-782.

Zhou, B., and Wen, J. F., 2007. Abnormality of summertime precipitation od Eastern China and general circulation with LFO in 1998. *Journal of Applied Meteorological Science*, **18** (2): 129-136.

Zhou, Z., Li, Y. D., Lin, M. X., Chen, D. X., Xu, H., and Luo, T. S., 2009. Preliminary study on climatic abrupt change and anomaly of tropical mountain rainforest from 1980 to 2005 in Jianfengling, Hainan Province. *Journal of Meteorology and Environment*, **25** (3): 66-72.

Zieger, S., 2010. Long term trends in ocean wind speed and wave height. PhD thesis. Swinburne University of Technology, Centre for Sustainable Infrastructure, Melbourne, Australia.

Zieger, S., Babanin, A. V., and Young, I. R., 2014. Changes in ocean surface winds with a focus on trends of regional and monthly mean values. *Deep Sea Research Part I*, **86**: 56-67.

(Edited by Xie Jun)

?1994-2017 China Academic Journal Electronic Publishing House. All rights reserved. http://www.cnki.net